Impact of an uncertain structural model on geothermal reservoir simulations

Jan Niederau[1], Henrik Büsing[1], Christoph Clauser[1], Tomi Jusri[2], Ivano Dini[3], Ruggero Bertani[4]

[1] Institute for Applied Geophysics and Geothermal Energy, E.ON Energy Research Center, RWTH Aachen University, Germany

[2] Institute of Geophysics and Geoinformatics, TU Bergakademie Freiberg, Freiberg, Germany

[3] Enel Green Power, Via Andrea Pisano 120, 56122 Pisa, Italy

jniederau@eonerc.rwth-aachen.de

Keywords: structural modelling, K horizon, numerical simulation, uncertainty assessment.

GLOSSARY

ϕ	Porosity
$\rho_{w,n}$	Density wetting phase, non-wetting phase [kg m^{-3}]
$S_{w,n}$	Saturation **w**etting phase, **n**on-wetting phase, with $S_w + S_n = 1$
t	Time [s]
$k_{r,w,n}$	Relative permeability of **w**etting phase, **n**on-wetting phase
$\boldsymbol{k}$	Permeability tensor [m²]
$p_{w,n}$	Pressure of **w**etting phase, **n**on-wetting phase, with $p_c = p_n - p_w$
g	Gravitational acceleration [m s^{-2}]
q^w	Source term [kg m^{-3} s^{-1}]
$u_{w,n}$	Specific internal energy of **w**etting phase, **n**on-wetting phase [J kg^{-1}]
$h_{w,n}$	Specific enthalpy of the **w**etting phase, **n**on-wetting phase [J kg^{-1}]
c_s	Specific heat capacity of the porous matrix [W kg^{-1} K^{-1}]
λ_{pm}	Tensor of mean thermal conductivity of the filled **p**orous **m**atrix [W m^{-1} K^{-1}]
q^h	Heat generation term [W m^{-3}]

ABSTRACT

Numerical reservoir models are usually based on geological and structural models. Geological and geophysical input for structural models has varying degrees of uncertainty, making the structural model itself uncertain. Usually, however, one single structural model is used for subsequent numerical simulations. We study an ensemble of different, but equally likely structures of a characteristic of geothermal reservoir systems in Tuscany, the K horizon. This horizon is a prominent seismic reflector and usually regarded as a 450 °C isotherm. Here, we present a workflow for assessing the impact of the structural uncertainty of the K horizon. By varying the structure of the K horizon within bounds of its uncertainty, we generate different structural models, which will be used for subsequent hydrothermal simulations. Comparison of simulation results to measured bottom-hole temperatures enables rejecting unlikely K horizon structures, thus reducing the amount of likely structures to a smaller ensemble which fit the temperature data.

1. INTRODUCTION

Most geothermal reservoir systems in Tuscany are characterised by young (Pliocene to Quaternary) intrusive bodies, acting as a primary heat source (Baldi et al., 1995; Batini et al., 2003, Brogi et al., 2005). A strong seismic reflector, the K horizon, correlates with the shape of the heat source, making the confidence in its modelled structure important.
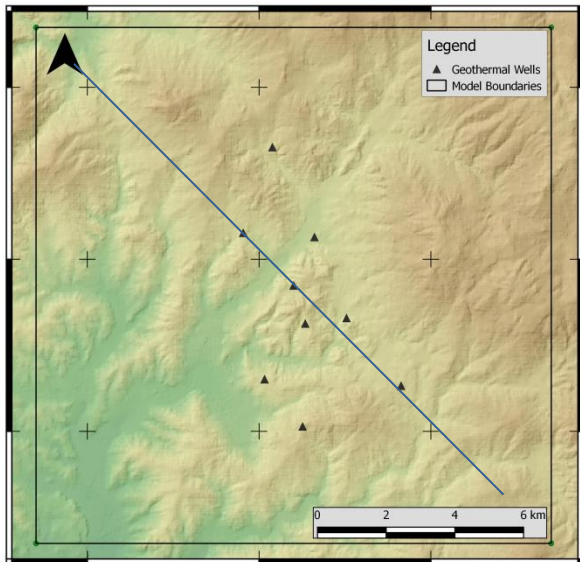
Figure 1: Topographic map of the model area in Tuscany. Black triangles indicate geothermal wells with data, the blue line the profile of the 2D numerical model ensemble assessed in this study.

Super-critical (*p,T*) conditions are expected to be present at and above the aforementioned K horizon, the primary heat source of the geothermal reservoir system. Consequently, the depth of the K horizon is assumed to be a controlling factor on the (*p,T*) condtions in the reservoir system. Assessing how the uncertainty in structure of the K horizon affects hydrothermal models of the reservoir system is therefore of great importance. Here, we present an approach for evaluating, and minimising an ensemble of possible K horizon structures, allowing for a statement on the uncertainty of the resulting numerical models. As these models provide an estimate of the regional temperature field and flow system, knowledge about their uncertainty is crucial.

2. GEOLOGICAL FRAMEWORK

The northern Apennines are a major fold-and-thrust belt originating from collision of the Adriatic microplate and the European Plate. During that compressional phase, eastward stacking of the several tectono-stratigraphic units took place (Brogi et al., 2005). This stacked sequence of sedimentary to meta-sedimentary rocks (sedimentary complex) comprises: (i) Miocene to Quaterny sediments, filling relatively young tectonic graben systems, (ii) The Ligurian & Subligurian Complexes, existing of remnants of the oceanic crust and flysch; (iii) the Tuscan Nappe sequence, consisting of continental sediments, to evaporites and turbiditic units. They represent a retrogradational sequence and are often tectonically laminated, with spatially varying thicknesses (Bertini et al., 2006), (iv) the Tectonic Wedge complex, consisting of alternating layers of quartzite, phyllite, carbonates and evaporates. Layers in the Tectonic Wedge complex are strongly fractured and pose the upper reservoir in the Larderello geothermal system (Bertini et al., 2006). Lithologies below the stacked

sedimentary complex are commonly referred to as the Tuscan Metamorphic Complex (Batini et al. 2003). Metamorphic lithologies within this complex range from meta-sandstones over phyllites to gneiss. Within the metamorphic complex is a highly permeable zone, usually referred to as the deep reservoir, lower reservoir H horizon (Bertani et al., 2005; Bertini et al., 2006). At greater depths, intruded magmatic bodies cause high-temperature/low-pressure metamorphism, and also pose the primary heat source in the studied geothermal system. Attributed to the intrusions in the lower part of the metamorphic complex is a discontinuous horizon, highly reflective in seismic data. This horizon is called the K horizon, whose origin has been discussed by various authors (e.g., Gianelli et al., 1997; Batini et al., 2003, Bertini et al., 2006). The tectono-stratigraphic pile is schematically shown in Figure 2.
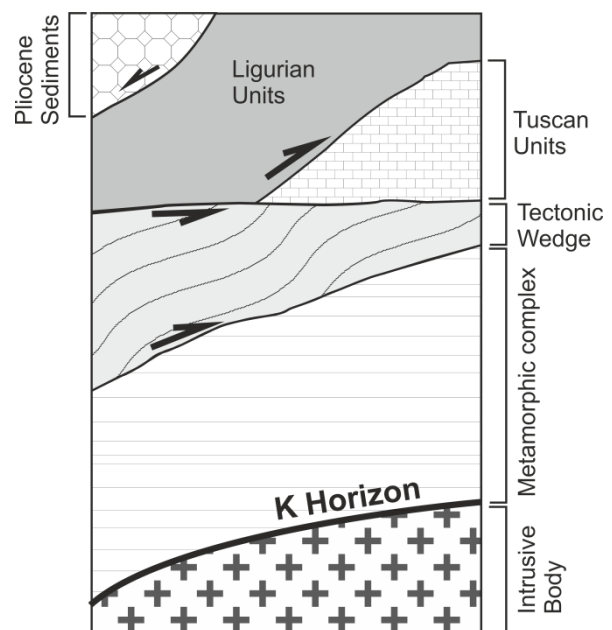

Figure 2: Schematic stratigraphic column in the assessed area. Within the metamorphic complex is a highly permeable fractured zone (modified from Ebigbo et al., 2016).

2.1 K horizon

The structure of the K horizon is often associated with the base of the geothermal system, i.e. its heat source (Romagnoli et al., 2010; Ebigbo et al., 2016). Although the K horizon marks a strong and dominant reflector in seismic data, its signal strength can vary considerably and it may show local ambiguities (Riedel et al., 2015). Ebigbo et al. (2016) assessed the influence of an uncertain structure and temperature of the K horizon on hydrothermal models. They show that a hydrothermal model is especially sensitive to the temperature of the K horizon, but to a lesser degree also to its structure. Though they study a different location in Tuscany, their findings also apply to the reservoir studied in this work. As the K horizon is shallower in the geothermal system presented in this paper, changes in its structure may have a bigger influence on simulation results.
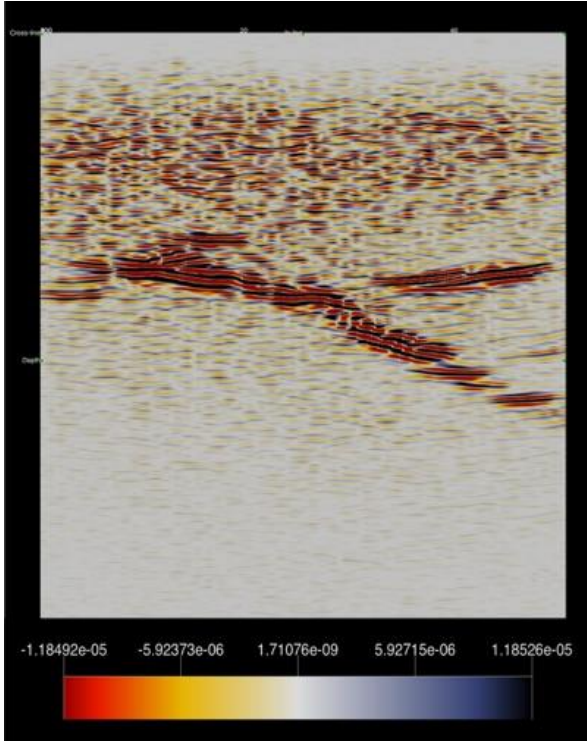
Figure 3: Seismic section from the study area. The strong reflectors are correlated to the K horizon (From Jusri et al., 2016).

Figure 3 shows an excerpt of a seismic section in the model area. The assumed K horizon is visible by its strong seismic reflections. However, the thickness of the reflector gives rise to a possible uncertainty in interpretation. Further, the branching visible in the right part of the image allows for two different interpretations of the structure of the K horizon: following the upper reflector, or following the lower reflector in the right part.

3. METHODS

In the following section, we'll address the modelling approach taken in this study, as well as briefly describe the main equations solved in the numerical model.

3.1 Mathematical Model

The fundamental model used is based on one mass-, and one energy conservation equation for a single component (water). In the study area presented, water exists as steam.

Transport of mass balance is calculated by the mass balance (symbols and units explained in the glossary):

$$\phi\frac{\partial(\varrho_{\mathrm{w}}S_{\mathrm{w}})}{\partial t} \quad + \quad \phi\frac{\partial(\varrho_{\mathrm{n}}S_{\mathrm{n}})}{\partial t} \qquad\qquad [1]$$

$$- \quad \nabla\cdot\left(\frac{k_{\mathrm{r,w}}}{\mu_{\mathrm{w}}}\varrho_{\mathrm{w}}\mathbf{K}\left(\nabla p_{\mathrm{w}}-\varrho_{\mathrm{w}}\mathbf{g}\right)\right)$$

$$- \quad \nabla\cdot\left(\frac{k_{\mathrm{r,g}}}{\mu_{\mathrm{n}}}\varrho_{\mathrm{n}}\mathbf{K}\left(\nabla p_{\mathrm{n}}-\varrho_{\mathrm{n}}\mathbf{g}\right)\right) \quad = \quad q^{\mathrm{w}}$$

Two phases are taken into account by considering saturations (S_w, and S_n), as well as relative permeabilities ($k_{w,r}$, and $k_{n,r}$).

Similarly to the mass balance equation, heat transport can be described by the energy balance equation:

$$\phi\frac{\partial(\varrho_{\mathrm{w}}u_{\mathrm{w}}S_{\mathrm{w}})}{\partial t} \quad + \quad \phi\frac{\partial(\varrho_{\mathrm{n}}u_{\mathrm{n}}S_{\mathrm{n}})}{\partial t}+(1-\phi)\frac{\partial(\varrho_{\mathrm{s}}c_{\mathrm{s}}T)}{\partial t} \qquad [2]$$

$$- \quad \nabla\cdot\left(\frac{k_{\mathrm{r,w}}}{\mu_{\mathrm{w}}}\varrho_{\mathrm{w}}h_{\mathrm{w}}\mathbf{K}\left(\nabla p_{\mathrm{w}}-\varrho_{\mathrm{w}}\mathbf{g}\right)\right)$$

$$- \quad \nabla\cdot\left(\frac{k_{\mathrm{r,g}}}{\mu_{\mathrm{n}}}\varrho_{\mathrm{n}}h_{\mathrm{n}}\mathbf{K}\left(\nabla p_{\mathrm{n}}-\varrho_{\mathrm{n}}\mathbf{g}\right)\right)$$

$$- \quad \nabla\cdot(\lambda_{\mathrm{pm}}\nabla T)=q^{\mathrm{h}}.$$

As advective and conductive heat transport are considered, equation [2] also contains Fourier's law for heat conduction. Effective values for a phase-filled porous media (e.g. λ_{pm}) are calculated using the geometric mean:

$$\lambda_{pm} = \prod \lambda_i^{n_i} \qquad [3]$$

3.2 Workflow and rejection algorithm

For assessing the impact of the K horizon structure on the resulting hydrothermal model, we established the workflow, schematically shown in Figure 4. First, a 2D ensemble of different possible K horizon structures is created. The ensemble comprises 700 realisations of the cross section indicated in figure 1. It is generated by considering the mean values and standard deviations listed in table 1. The standard deviation in depth of the K horizon is adapted from a study by Riedel et al (2015) who estimated the depth of the K horizon to vary by ± 150 m (σ) in a different reservoir system in Tuscany. In a second step, the generated structural models are used as geometries in our hydrothermal models, where the coupled energy- and mass balance equations (equation [2] and equation [3]) are solved. We call this ensemble of hydrothermal models the *prior distribution*. By using a Markov Chain Monte Carlo method (MCMC), we reject realisations from the *prior distribution* by comparing their temperature results with measured bottom hole temperatures (BHTs).

Table 1: Mean and standard deviations connected to depth and inclination of the K horizon.

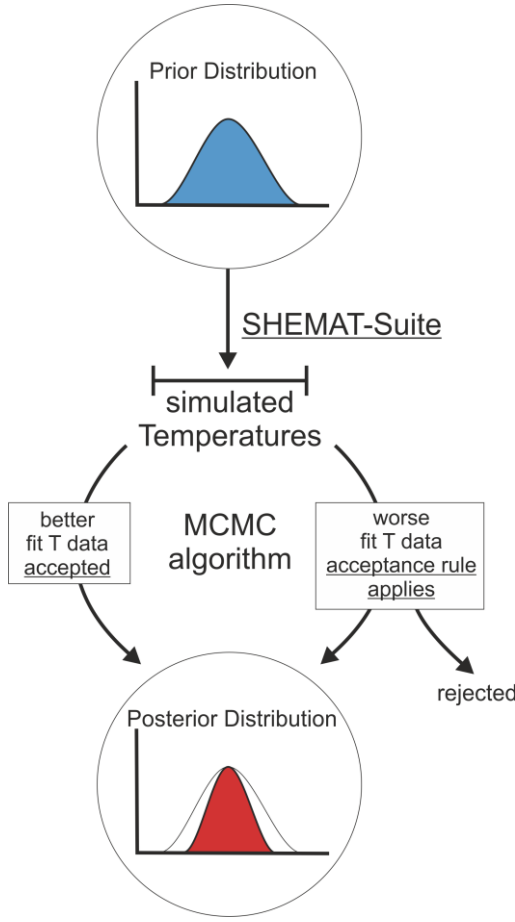| Type	Mean	Stdev σ
Interface K horizon	-4160 m	150 m
Dip K horizon north	35.6 °	10 °
Dip K horizon south	25.56 °	10 °

Figure 4: Schematic sketch of the workflow used.

In the following, the MCMC algorithm will be briefly described.

Metropolis Algorithm

Bayes' theorem is a simple, yet powerful statement about the probability of a hypothesis of a model M to be true, given information D about it, quantified in the form of a conditional probability $p(M|D)$. In most practical applications, this term is now known, but can be calculated through an application of Bayes' equation (Downey, 2013):

$$p(M|D) = \frac{p(M)p(D|M)}{p(D)} \qquad [4]$$

The notation $p(M)$ states the probability of a model to be true without considering further information. This is denoted as prior probability. Considering information, e.g. temperature measurements in case of geothermal systems, we aim to determine the posterior model probability as the conditional probability $p(M|D)$. There are two further terms in equation [4]: $p(D|M)$ is called the likelihood and represents the likelihood of a model to be generated by the data. Analogous, $p(D)$ represents the probability of the data under any model, also called evidence.

We use here a Metropolis algorithm, which conditions a Markov Chain by a probabilistic rule (Tarantola, 2005). Basically, the Metropolis algorithm applies two steps: a proposal step, and an acceptance step. In the

proposal step, a sample (x_j) (i.e. model realisation) is proposed on the basis of an accepted previous model state. Then, a sample (x_j) is accepted or rejected on the basis of a comparison to the current sample (x_i). This is done with an acceptance rule, which, in case of normal distributions, can be written as:

$$p_{accept} = \begin{cases} \exp\left(-\dfrac{S(x_j) - S(x_i)}{u_T}\right), S(x_i) < S(x_j) \\ 1 \qquad\qquad\qquad\qquad , otherwise \end{cases} \qquad [5]$$

where $S(x_{i,j})$ is the root-mean-square error from the samples (x_i) and (x_j), and u_T is the error of our temperature data. The error of temperature measurements in our calibration boreholes are of the same magnitude as temperature measurement errors stated in Ebigbo et al (2016). u_T is estimated by using error propagation from various error sources, e.g. measurement error and discretisation error.

Information entropy

For visualising the uncertainty of the K horizon shape, we use an information entropy method, which is based on the Shannon Entropy (Shannon, 1948). In our model context, we vary just the shape of the K horizon randomly around a mean and a standard deviation. Thus, a cell in our model can either belong to the unit below the K horizon, or to the one above it. Consequently, there are two possible outcomes. The measure of information entropy indicates the amount of missing information in bits, and here applied in a spatial context (Wellmann and Regenauer-Lieb, 2012). Information entropy for discrete systems can be calculated as:

$$H(X) = -\sum_{i=1}^{n} p_i \, log_2 p_i \qquad [6]$$

Where X is a random variable with n possible outcomes $x_i, \dots x_n$ and corresponding probabilities p_i. $H(X)$ is the resulting information entropy value in bits (Wellmann, 2013).

4. STRUCTURAL MODEL

The structural model of the geothermal reservoir system is based on the main tectono-stratigraphic units shown in Figure 2, plus a deep reservoir body, so seven units in total. It is constructed from seismic data, borehole data, and geological maps and cross-sections. There are around 55 boreholes with depths between 100 m and 800 m in the study area. Consequently, the upper part of the model, comprising the sedimentary units down to a depth of 1000 m is well resolved. The model certainty decreases with depth, due to less data available. Information about the deeper structure comes from 9 deep boreholes and a 3D seismic dataset.

The seven units in the structural model are constructed by an implicit modelling approach, implemented in the software GeoModeller (Lajaunie et al., 1997). Surface topography in the model was built from a

30 m DEM from the Shuttle Radar Topographic Mission (SRTM), distributed by the USGS.

The tectonic-wedge unit is strongly varying in its thickness over the model domain. It consists of a fault bound repetition of evaporates, carbonates, and metamorphic rocks, as deduced from borehole logs. Those repetitions are impossible to cross-correlate between boreholes. Thus the tectonic-wedge is modelled as one unit in our structural model, representative for the lithologic repetition described above.

The ensemble of different K horizon geometries described in subsection 3.3 is generated from a cross section, indicated in figure 1. The ensemble of different 2D geometrical models is then transferred in numerical models.

5. NUMERICAL MODEL

The 2D numerical model ensemble generated from the structural model ensemble is simulated using the code SHEMAT-Suite (equations [1] and [2]). Each model is discretised in a hexahedral grid of $500 \times 1 \times 200$ cells (in x, y, and z direction). Cell dimensions are 35 m in x direction and 45 m in z direction.

5.1 Boundary conditions and initial values

The top temperature boundary condition in our model depends on air temperature, i.e. topography, with an average temperature gradient of 1 K for 184 m of altitude (Claps et al., 2008). The top pressure boundary condition in our model is atmospheric (0.101325 MPa). This implicates that our whole lithologic column is water saturated, i.e. the groundwater table coincides with surface topography. For lateral pressure boundary conditions we use hydrostatic pressure.

The K horizon is assumed to be isothermal with a temperature of 450 °C (Liotta and Ranalli, 1999; Batini et al., 2003). Lateral boundary conditions for temperature are used from a conductive steady state model.

Initial values of temperature and pressure are obtained from a steady state solution of a model with a K horizon geometry, resembling the mean of the generated ensemble.

5.2 Petrophysical parameters

Petrophysical parameters of the main units in our model are obtained from laboratory measurements for the metamorphic complex. For the other units, values were obtained from Ebigbo et al (2016), who assessed the petrophysical properties for parts of the tectonic wedge unit and the metamorphic complex by borehole log analysis and laboratory measurements. They refer to the tectonic wedge unit as the Burano unit. As the tectonic wedge unit in our study is less dominated by the anhydritic Burano formation, its thermal conductivity is smaller.

Table 2: Main input parameter for the lithological units in the numerical model. Note the high thermal conductivity (TC) of the Sub K Horizon unit is chosen to get 450 °C at the K Horizon.

Unit	Porosity	Permeability $[10^{-15}$ m²]	TC (sat.) $[W\ m^{-1}\ K^{-1}]$
Ligurian Units	0.05	10^{-3}	2.24
Tuscan Units	0.05	1	2.7
Tectonic Wedge	0.05	$0.15 - 0.015$	3.72
Met. Complex	0.03	0.01	3.2
Sub K Horizon	0	10^{-5}	10^2

The thermal conductivity value of the metamorphic complex was assessed on seven core samples which come from four different boreholes in the study area. The value presented in table 2 is a mean value of the measurements.

6. PRELIMINARY RESULTS

Up to now, the prior distribution of different K horizon structures was generated using GeoModeller. This model ensemble is currently transferred to numerical models, which are solved in SHEMAT-Suite. Figure 5 shows a cross-section through one of the model scenarios, as well as a visualisation of the information entropy as a measure of uncertainty of the K horizon in the prior ensemble.
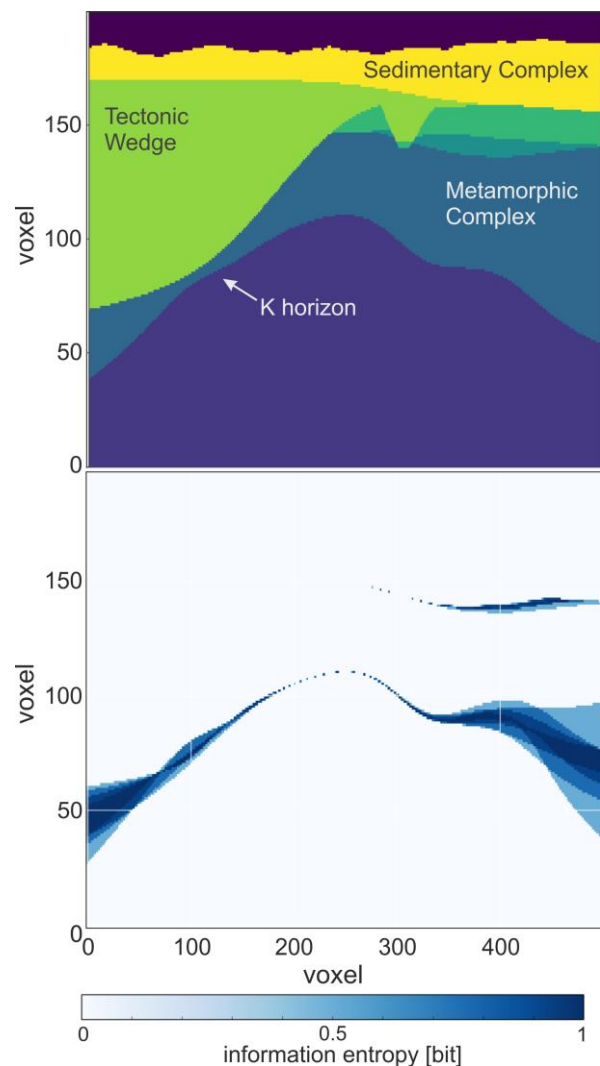
Figure 5: Top: Cross-section through the model, showing a possible structure of the K horizon. Bottom: Information entropy of the prior model ensemble, calculated with eq [6].

The upper image in Figure 5 shows a cross section through a single realisation of the structural model, with a possible shape of the K horizon. In total, we calculated an ensemble of 700 equally likely shapes of the K horizon. A probability map of the information entropy of the K horizon over the whole ensemble shows that especially the change in the angle of the dipping flanks has a significant effect on the shape of the K horizon. The central part, which is also the shallowest, does not vary substantially in its structure.

Currently, the 700 structural models are transferred in numerical models, and simulations are performed. Once the simulations are finished, we will use the rejection algorithm described in subsection 3.3 to obtain a posterior distribution of possible K horizon shapes in this 2D model.

It has to be noted that our approach does not cover all sources of uncertainty which influence simulated temperatures. For instance, thermal conductivity tensors within the metamorphic complex differ in magnitude, and show a varying degree of anisotropy. The spatial variation of petrophysical properties, such as thermal conductivity or permeability is a source of uncertainty which is not covered by our approach. However, the focus of our study is to assess the impact of uncertain structure on the simulated temperature field. As such, consideration of various sources of uncertainty may hamper the interpretation of our results.

Further, the ensemble size (700 realisations) can be discussed. It is not likely that the whole probability space is covered by our ensemble, and that the prior distribution has to be bigger. The approach is further limited by computational feasibility, as each model realisation has to be solved for pressure and enthalpy, temperature respectively.

7. CONCLUSIONS

In this study, we vary the structure of the K horizon, a key characteristic of an assessed geothermal reservoir system in Tuscany. The shape of the K horizon is deduced from seismics, which are connected to a certain uncertainty. We create a workflow to account for this uncertainty by creating an ensemble of different K horizon structures with equal probability. In ongoing work, this probability is conditioned by applying Bayes' theorem, rejecting K horizon structures, which do not coincide with measured bottom-hole temperatures. Finally, this yields a smaller posterior ensemble of possible K horizon structures.

REFERENCES

Baldi, P., Bellani, S., Ceccarelli, A., Fiordelisi, A., Squarci, P., and Taffi, L.: Geothermal anomalies and structural features of southern Tuscany. In *World Geothermal Congress Proceedings Florence*, 1287-1291, (1995).

Batini, F., Brogi, A., Lazzarotto, A., Liotta, D., and Pandeli, E.: Geological features of Larderello-Travale and Mt. Amiata geothermal areas (southern Tuscany, Italy). *Episodes*, *26*(3), 239-244, (2003).

Bertani, R., Bertini, G., Cappetti, G., Fiordelisi, A., and Marocco, B. M.: An update of the Larderello-Travale/Radicondoli deep geothermal system. In *Proceedings* (pp. 24-29), (2005).

Bertini, G., Casini, M., Gianelli, G., and Pandeli, E.: Geological structure of a long-living geothermal system, Larderello, Italy. *Terra Nova*, *18*(3), 163-169, (2006).

Brogi, A., Lazzarotto, A., Liotta, D., Ranalli, G., and CROP18 Working Group.: Crustal structures in the geothermal areas of southern Tuscany (Italy): insights from the CROP 18 deep seismic reflection lines. *Journal of Volcanology and Geothermal Research*, *148*(1), 60-80, (2005).

Claps, P., Giordano, P., and Laguardia, G.: Spatial distribution of the average air temperatures in Italy: quantitative analysis. *Journal of hydrologic engineering*, *13*(4), 242-249, (2008).

Downey, A.: Think Bayes. *O'Reilly Media, Inc*, Sebastopol, (2013).

Ebigbo, A., Niederau, J., Marquart, G., Dini, I., Thorwart, M., Rabbel, W., Pechnig, R., Bertani, R., and Clauser, C.: Influence of depth, temperature, and structure of a crustal heat source on the geothermal reservoirs of Tuscany: numerical modelling and sensitivity study. *Geothermal Energy*, *4*(1), 1, (2016).

Gianelli, G., Manzella, A., and Puxeddu, M.: Crustal models of the geothermal areas of southern Tuscany (Italy). *Tectonophysics*, *281*(3), 221-239, (1997).

Jusri, T., Bertani, R., Dini, I., Ciuffi, S., and Buske, S.: Reprocessing of a 3D seismic data set from a geothermal field in mid-southern Tuscany (Italy), *Poster at annual meeting DGG*, Münster, 14. – 17. March, (2016).

Lajaunie, C., Courrioux, G., and Manuel, L.: Foliation fields and 3D cartography in geology: principles of a method based on potential interpolation. *Mathematical Geology*, *29*(4), 571-584, (1997).

Liotta, D., and Ranalli, G.: Correlation between seismic reflectivity and rheology in extended lithosphere: southern Tuscany, inner Northern Apennines, Italy. *Tectonophysics*, *315*(1), 109-122, (1999).

Riedel, M., Dutsch, C., Alexandrakis, C., Dini, I., Ciuffi, S., and Buske, S.: Seismic depth imaging of a geothermal system in Southern Tuscany. *Geophysical Prospecting*, *63*(4), 957-974, (2015).

Romagnoli, P., Arias, A., Barelli, A., Cei, M., and Casini, M.: An updated numerical model of the Larderello–Travale geothermal system, Italy. *Geothermics*, *39*(4), 292-313, (2010).

Sambridge, M., and Mosegaard, K.: Monte Carlo methods in geophysical inverse problems. *Reviews of Geophysics*, *40*(3), (2002).

Tarantola, A.: Inverse Problem Theory and Methods for Model Parameter Estimation, *Society for Industrial and Applied Mathematics*, Philadelphia, (2005).

Wellmann, J.F.: Information Theory for Correlation Analysis and Estimation of Uncertainty Reduction in Maps and Models. *Entropy*, 15, 1464-1485, (2013).

Wellmann, J. F., and Regenauer-Lieb, K.: Uncertainties have a meaning: Information entropy as a quality measure for 3-D geological models. *Tectonophysics*, *526*, 207-216, (2012).